

NOTICE CONCERNING COPYRIGHT RESTRICTIONS

This document may contain copyrighted materials. These materials have been made available for use in research, teaching, and private study, but may not be used for any commercial purpose. Users may not otherwise copy, reproduce, retransmit, distribute, publish, commercially exploit or otherwise transfer any material.

The copyright law of the United States (Title 17, United States Code) governs the making of photocopies or other reproductions of copyrighted material.

Under certain conditions specified in the law, libraries and archives are authorized to furnish a photocopy or other reproduction. One of these specific conditions is that the photocopy or reproduction is not to be "used for any purpose other than private study, scholarship, or research." If a user makes a request for, or later uses, a photocopy or reproduction for purposes in excess of "fair use," that user may be liable for copyright infringement.

This institution reserves the right to refuse to accept a copying order if, in its judgment, fulfillment of the order would involve violation of copyright law.

From the Tectonic and Structural Analysis towards a Fracture Network Model for Hydraulically Modeling the Soultz EGS (France)

M. Peter-Borie and S. Gentier

BRGM GTH/RG, Orléans, France

m.peter@brgm.fr

Keywords

EGS, Soultz-sous-Forêts, fracture network, Terzaghi's correction factor, density, length, line survey

ABSTRACT

In order to simulate the hydraulic behavior of the Soultz-sous-Forêts EGS, a 3D flow and transport model with a DFN approach (Discrete Fracture Network) is built. A fundamental step of this modeling is the construction of the 3D fracture network. This paper deals with the fracture network construction from available data and data treatment with probabilistic and statistical approaches in consistence with geological setting. Five fracture sets have been defined in accordance with tectonic history and characterized in terms of orientation (mean and dispersion). Length and density are key points of 3D network: couples fracture density/fracture length are estimated from probability of fracture/well intersection and observed data. Although tectonic history gives information on the order of magnitude of the fracture length, geological settings do not allow the efficient hydraulic fracture size to be constrained.

Introduction

To understand the Soultz-Sous-Forêts EGS (Enhanced Geothermal System) circulation paths in the fractured granitic basement between the three wells GPK2, GPK3 and GPK4, a hydraulic model of the reservoir is built using Discrete Fracture Network (DFN) approach. A key point of the model is the construction of a numeric fracture network that allows the observed behavior of the efficient hydraulic fracture network to be reproduced from hydraulic and tracer tests. The numeric fracture network is composed by several disc sets, assimilated to fracture sets; each of them is characterized by its mean orientation and its orientation dispersion, its length probability distribution and its density. An endless number of networks can be found, but the number of solutions can be restrained by statistical and probabilistic analysis of the available data and structural and tectonic constrains.

Some fracture data are available and can give information on the efficient hydraulic fracture network; however, it comes up against several biases, uncertainties and unknowns as the data have been acquired in the wells from mainly Ultrasonic Borehole Imager and as no information about permeability of the detected fractures is available.

Structural and tectonic constraints, closely linked to regional tectonic history, can give intervals for the number of fracture sets, their orientation, their length, density and information about permeability.

This paper presents the analysis methods used to define the main characteristics of a physically and geologically consistent fracture network of Soultz-sous-Forêts granitic basement. They involve statistical and probabilistic analysis, bias corrections of 1D fracture data acquired in the wells and structural and tectonic knowledge. The acquired characteristics are the basis for finding one fracture network that has been calibrated and validated by hydraulic modeling presented in the companion paper Gentier *et al.* (2011). After setting the fracture data in their geological and measurement context, the different fracture sets are studied from statistical analysis and in relation to the tectonic history. The density and the length of the fractures are then estimated from probabilistic studies and constrained by the geological knowledge.

Geological Context

The Soultz-sous-Forêts EGS is located near the western boundary fault of the Upper Rhine Graben, in northeastern France, above a thermal anomaly associated with a horst structure (Figure 1a). This geothermal system exploits the heat tank, which is the granitic basement rocks lying under 1400 m of sedimentary deposits, through forced fluid circulation in a fracture network between wells drilled to 5000 m depth where the temperature reaches 200°C.

The fracture network in the granites from Soultz-sous-Forêts is the result of a succession of deformations through time. As the granitic intrusions were emplaced and cooled down in the Visean time (≈ 330 Myr), all the tectonic phases that occurred between the Hercynian orogeny (Autunian compression, ≈ 280 Myr) to recent alpine compression, including the Oligocene Rhine Graben rifting,

have consequences on the actual efficient hydraulic fracture network. Actually, some tectonic phases create discontinuity sets while others reactivate pre-existing fractures under different stress states (Schumacher, 2002; Edel *et al.*, 2006). Evolution of the stress state leads to a change of the void geometry that results in modifying the fracture permeability (Gentier *et al.*, 1997). A large part of the fracturing observed in the granites from Soutz-sous-Forêts is related to the Hercynian orogeny and particularly to Carboniferous and Permian phases of wrench tectonics (Ziegler, 1990). Schumacher (2002) and Edel *et al.* (2006), among others, underline the role of the reactivation of the Hercynian faults during the subsequent tectonic phases.

Rough Data

Five deep wells have been drilled into the granite basement: EPS1 (≈2200 m depth; fully cored), GPK1 (≈3600 m depth), GPK2 (≈5100 m depth), GPK3 (≈5000 m depth) and GPK4 (≈5000 m depth; Figure 1). The different circulation tests have been initially performed between GPK1 and GPK2 (top-part), and then, between the wells of the triplet formed by GPK2 (bottom-part), GPK3 and GPK4. These three wells have been drilled from the same drilling pad and hence are deviated to reach, at 5000 m depth, a distance of about 700 m along a N165° direction between the wells.

Wells GPK1, GPK3 and GPK4 were completely logged in the granite, whereas in GPK2, due to logging problem (discontinuity shearing that shifts the borehole, preventing the insertion of the tools), the log stopped at 3800 m and thus no images were acquired in the bottom part of the well between 3800 and 5100 m. More than 6000 fractures have been detected on acoustic image logs (from mainly Ultrasonic Borehole Imager) and measured in the granite (Dezayes *et al.*, 2005b). But these fractures cannot be directly used to estimate the efficient hydraulic network: it comes up against several biases, uncertainties and unknowns (Figure 2):

- The detection of fractures in the well is biased by the well

orientation: all fracture orientations are not proportionately intersected as the intersection probability decreases while the angle between the sampling line and the normal to a discontinuity increases.

- The efficient hydraulic fracture network and the detected fracture network are two different subsets of the global fracture network:
 - Other studies of permeable fractures in fractured rock mass show that the efficient hydraulic fracture network could represent about 10% of the global fracture network (Billiaux, 1990).
 - Comparison between Ultrasonic Borehole Imager (UBI) fractures data and fractures from cores in EPS1 show that the detected fracture network is a subset representing about 20% of the global fracture network (Gentier, 1997). In particular, discrete fractures thinner than 1 mm are not properly imaged, discrete fractures that are less spaced than 5 mm appear only as one single trace, and the roughness of the borehole wall in altered granite section usually leads to a degradation of the image quality under-estimating the fracture trace number.
- Different fracture directional sets are probably not proportionally represented in the efficient hydraulic fracture network, nor in the detected fracture network. Furthermore, in each fracture set, the ratio of efficient hydraulic fractures is likely different of the ratio of detected fractures.
- Finally, measurements of fracture orientations have attached uncertainties as an error of ±2° in azimuth and in deviation is associated with the transformation of apparent measured orientations on borehole images in true orientations using the borehole azimuth and deviation measurements (Valley, 2007).

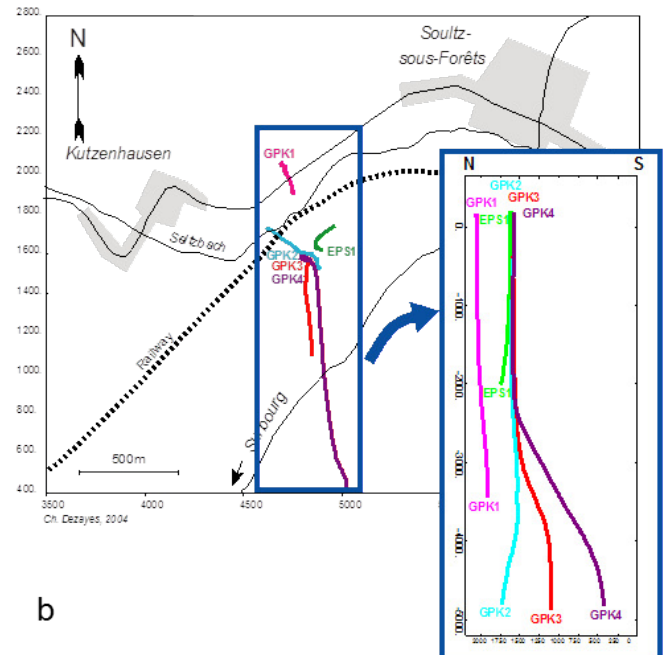
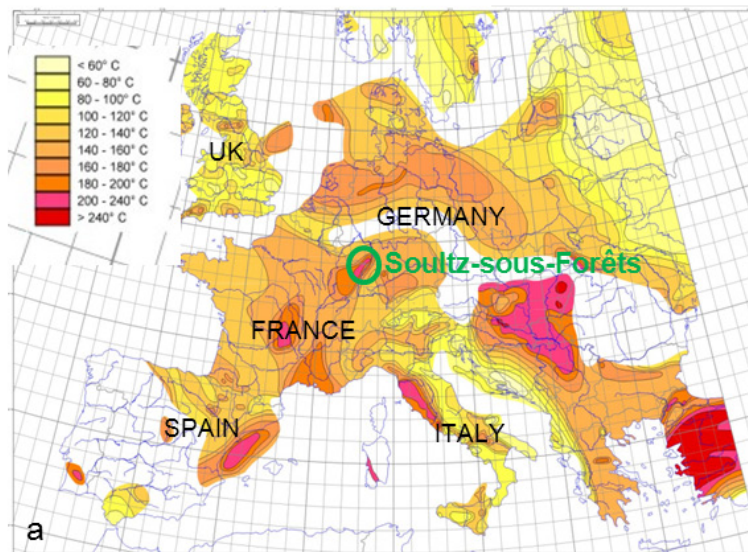
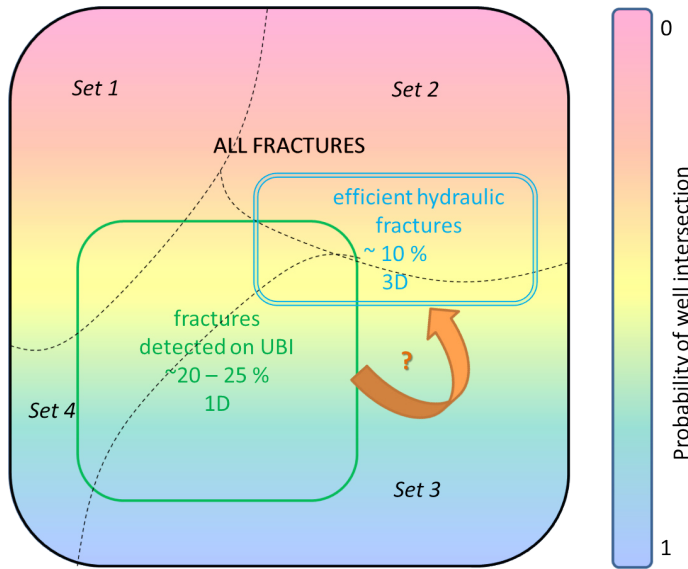


Figure 1. a) Map of temperature extrapolated at 5km depth in Europe (Hurtig *et al.*, 1992) and Soutz-sous-Forêts location ; b) Wells trajectory (plan and N-S section; Dezayes *et al.*, 2005a).



$$w = \frac{1}{\cos \delta} \tag{Eq 1}$$

When δ approaches 90° , w becomes very large; in this case, a single point could dominate the distribution pattern. Moreover, according to Yow (1987), an estimation of the error on the Terzaghi's correction factor ($w_{\epsilon, \max}$; Equation 2) can be expressed from the error ϵ associated with taking orientation measurements (about 2° , Valley, 2007):

$$w_{\epsilon, \max} = \left(\frac{\cos \delta}{\sin(90^\circ - \delta - \epsilon)} - 1 \right) \tag{Eq 2}$$

The error associated with high values of w is very important, more than 100% for $\delta > 88^\circ$. Thus, as recommended in Priest (1993), a maximum allowable weighting has been set. A maximum value of $w=10$ has been adopted in the presented study, corresponding to $\delta=84.3^\circ$ and to a maximum error of 20% associated with $\epsilon=2^\circ$. Figure 4 shows the evolution of the distribution of fracture orientation consequently to the adopted Terzaghi's weighting. Figure 5a and 4b show the diagram of contour-density from rough data (Figure 5a) and from weighted data (Figure 5b). The main impact of this weighting is the shift of dip values to higher values that is consistent with the fact that due to the well's trend, mainly vertical, the vertical fractures are underestimated (Figure 4a and b). Furthermore, fractures characterized by a dip direction:

- between 50° and 80° (strike between $N140^\circ$ and $N170^\circ$, NE-dipping),
- between 90° and 110° (strike between $N0^\circ$ and $N20^\circ$, E-dipping),
- between 180° and 230° (strike between $N90^\circ$ and $N140^\circ$, S and SW-dipping),

are slightly underestimated in rough data. On the contrary, fractures characterized by a dip direction comprised between 240° and 310° (strike between $N150^\circ$ and $N180^\circ$, W-dipping and $N0^\circ$ and $N40^\circ$, W-dipping) are slightly over-estimated (Figure 4a and c). Wells are thus favorably purposely oriented to intersect mainly N-S striking W-dipping fractures.

Statistical Analysis in Direction and Dip of the Fracture Network

The probability of intersection of a wellbore with a fracture depends on the relative orientations of the fracture and of the well (Figure 3). Thus, rough data do not allow the direct computation of all the fracture sets: fracture sets whose orientation is nearly parallel to the well are underestimated or skipped. One of the first to analyze this bias was Terzaghi (1965); he proposed a geometrical correction factor w (equation 1) based on the observed acute angle d between the sampling line (here, the well trajectory) and the normal to the discontinuity:

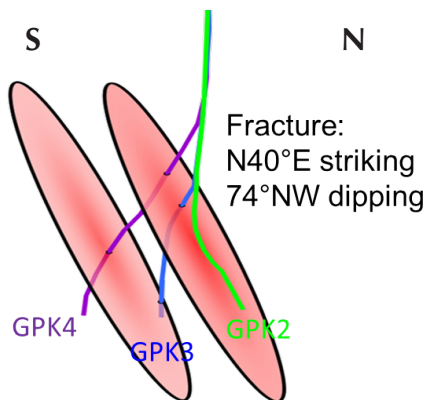


Figure 3. Illustration of the probability of intersection depending on well orientation through a schematic view, in a S-N cross-section, of the wells GPK4 and GPK3 that are favorably oriented to intersect a fracture $N40^\circ$ striking, 75° NW dipping, while GPK2 is not as the trend of the well bottom part is quite parallel to the fracture.

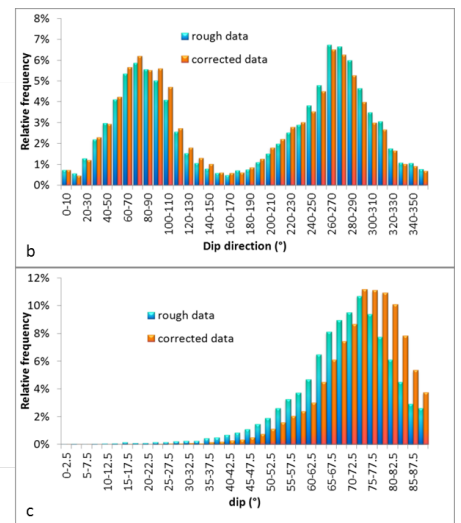
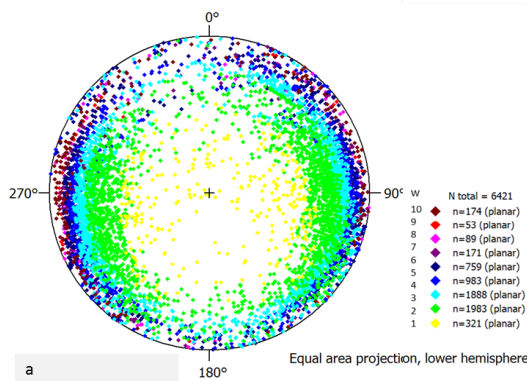


Figure 4. (a) Cloud of the normal to the 6421 fractures collected in the wells GPK1, 2, 3 and 4; colors refer to attributed weights from Terzaghi's correction. Evolution of the distribution of fracture dip direction (b) and dip (c) with the Terzaghi's correction weighting factor.

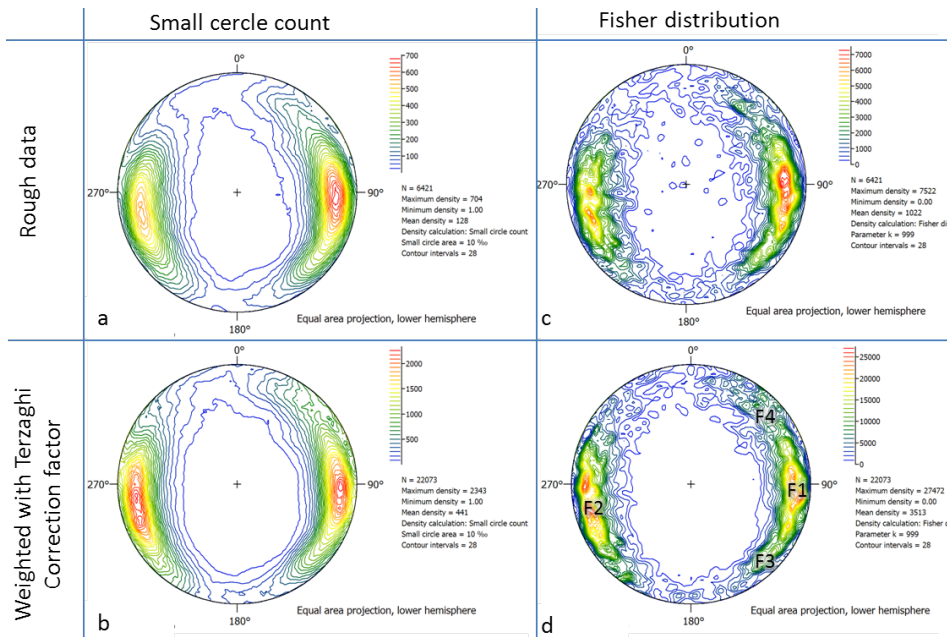


Figure 5. Density contour of the normal to the 6421 fractures reported on UBI image in GPK1, GPK2, GPK3 and GPK4 between 1300 and 5000 m depth. a. Classical computation on rough data (Small circle count); b. Classical density computation (small circle count) on weighted data (Terzaghi's correction factor); c. Fisher distribution density computation on rough data; Fisher distribution density computation on weighted data (Terzaghi's correction factor).

This computation method infers uncertainties in density estimation for fractures that are sub-parallel to well trend (mainly SE-NW-striking NE-dipping, NS-striking E-dipping and EW to SE-NW-striking SW-dipping; Figure 4a). In fact, the main consequence of an imposed threshold is to potentially underestimate the density of fractures characterized by a high value of δ . A measurement error ϵ of 2° may infer Terzaghi's correction factor incertitude from ± 1 to ± 2 for δ superior to 80° .

In order to avoid missing fracture sets due to density underestimation, a density calculation has been performed applying Fisher's distribution (1953). It defines with a parameter k that is a measure of a degree of clustering or degree of concentration within the population (Priest, 1993). To bring out sets of fractures that are represented by few entities and that are so presumably masked by numerous fractures of major sets, a maximal k value have been chosen ($k=999$; Figure 5c and d).

This analysis shows four fracture sets associated with the main modes of density (reported on Figure 5d):

- F1 set: N-S striking, W dipping,
- F2 set: NNW-SSE striking, E dipping; this set is involved with highly weighted data, the modal fracture is thus not well constrained,
- F3 set: NE-SW striking, NW dipping,
- F4 set: NW-SE striking, SW dipping; this set is also involved with highly weighted data, the modal fracture is thus not well constrained too.

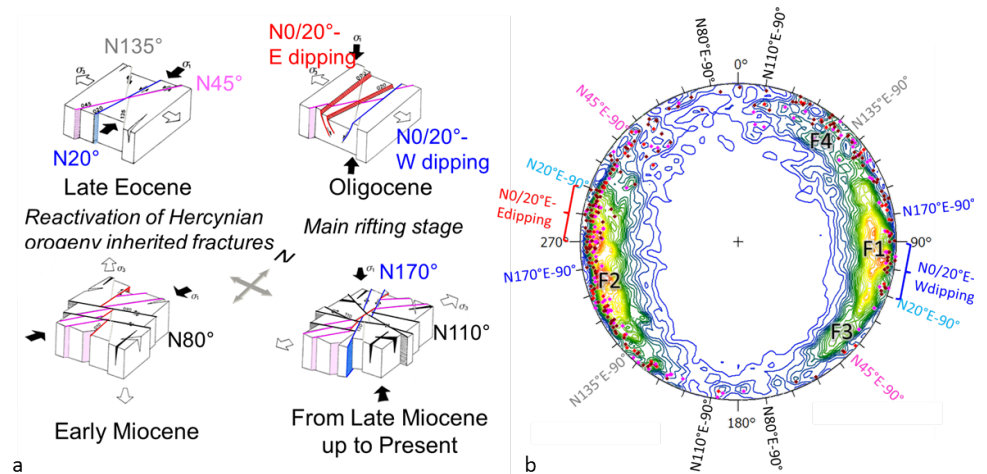


Figure 6. a) Cenozoic tectonic history of the Rhine Graben (modified from Valley, 2007); b) Fracture sets reported on density contour (see legend Figure 5) on Schmidt projection, and highly weighted fractures ($w \geq 8$) (see legend Figure 4)

These four fracture density modes are consistent with structure orientations observed regionally (Figure 6a and 5b):

- F1 set, mainly \sim N-S striking W dipping, is widely observed in the Rhine Graben and commonly interpreted as the result of the Oligocene deformation (N0/20° striking, W dipping). But this set could also be related:
 - to lower Carboniferous to Permian N20° sinistral faulting (Schumacher, 2002) reactivated during late Eocene,
 - to N170° sinistral strike-slip faults reactivated from late Miocene up to now under a NW-SE compression of the graben as a strike-slip system (Schumacher, 2002; Bergerat, 1985 and Villemin, 1986).
- F2 set, \sim NNW-SSE striking, E dipping, characterized by a high dispersion around the mean fracture orientation, is also commonly interpreted as the result of the Oligocene deformation (N0/20°-striking, E-dipping). But it could be considered as different sets gathering Hercynian N20° sinistral strike-slip and N135° dextral strike-slip reactivated during late Eocene and to N170° sinistral strike-slip faults. This F2 set is associated with a poor constraint density computation due to numerous highly weighted fractures.
- F3 and F4 sets, respectively NE-SW and NW-SE striking, are consistent with the Hercynian orientations observed regionally.

The fractures belonging to F1, F2, F3 and F4 sets have been delimited by contouring. The representative orientation and characteristics of the resultant vector of the normals to all fractures related to each set are given Table 1. For each set, the normal-

ized length of the mean vector perpendicular to the mean plane provides a measure of the degree of clustering within the set: as it approaches 1, each defined set is closely clustered. The dispersion of each set has been defined by adjusting a normal probability distribution characterized by a standard deviation value (Table 1).

Once the fractures belonging to these four fracture sets are removed, a fracture cloud still remains. It concerns, in particular, the N80° and N110° striking fractures that cannot be associated with a modal density (Figure 6b) but that can be related to tectonic sets. These fractures are mainly related to a value of $w=10$ (Terzaghi's correction factor) as they are characterized by an acute angle between the sampling line (here, the well trajectory) and the normal to the discontinuity $\delta > 84.3^\circ$. To reproduce this cloud and to compensate all the mis-weighted fracture orientations (mainly N80° and N110° striking fractures, but also many other fractures striking between N0° and N180°), a fifth set, F5, uniformly distributed from N0° to 180° striking, is created.

Table 1. Main statistical data of fracture sets.

Set of Fractures		F1	F2	F3	F4	F5
Strike and dip of the mean plane		N2°-70°W	N162°-70°ENE	N42°-74°NW	N129°-68°SW	N0° to 180° 70°
Standard deviation of the plane strike		16°	19°	6°	6°	
Standard deviation of the plane dip		7°	7°	3°	3°	9°
Distribution type (strike and dip)		normal	normal	normal	normal	Uniform (dip direction) – normal (dip)
Eigen vector	Cartesian coordinates	0.03, -0.94, -0.33	0.29, 0.89, -0.34	0.65, -0.71, -0.26	0.72, 0.59, 0.37	
	strike and dip	N272°-19°NW	N252°-19°	N132°-15°	N39°-21°	
Normalized length of the mean vector perpendicular to the mean plane		0.957	0.944	0.994	0.994	

From 1D Data to 3D Network

To define a 3D fracture network to model the Soultz-Sous-Forêts EGS reservoir hydraulic behavior using a 3D Discrete Fracture Network (DFN) approach, a volumetric density, spatially homogeneous or not, a length distribution and a shape are required for each fracture set. But, little or no information is available:

- The density which is directly measured along a well bore must be corrected of the well orientation and is probably not representative of the efficient hydraulic fracture network (Figure 2). In addition, it should be noticed that, although they have not been corrected from intersection probability, high concentration of fractures in limited depth intervals are observed and are interpreted as clusters (Genter *et al.*, 1997, Dezayes *et al.*, 2005)..
- As only data from well bores are available, no information on fracture shape and length is directly available. No outcrop of the studied granite exists that prevents studies of traces length produced by fracture intersections and rock face.

- In a completely blocky rock mass, where all fractures terminate at other fractures, the shapes will take the form of complex polygons whose geometry is governed by the locations of the bounding fractures (Priest, 1993). As fracture occurrence is often random, estimating the shape of each fracture is then impossible.

Assumptions are thus needed for the construction of the 3D fracture network used to model the Soultz-Sous-Forêts EGS reservoir hydraulic behavior:

- In view of the difficulties to estimate the fracture shape, a number of workers have adopted the simplifying assumption that discontinuities are circular (Priest, 1993). The same assumption is made in the used Discret Fracture Network approach: fractures are thus assimilated to circular discs.
 - A spatially homogeneous distribution of fractures is considered as hypothetical clusters in limited depth intervals cannot be delimited in 3D space.
 - As no geological arguments are available to differentiate efficient hydraulic fractures from impermeable fractures, in first approximation, the density of efficient hydraulic fractures is considered to be proportional to the detected fractures density.
- The first stage of the density estimation consists of studying the probability of intersection of each fracture orientation with the trajectory of each well.
- The study is focalized on the area involved in the hydraulic model presented in Gentier *et al.* (2011). We thus estimate the probability of intersection of the four main fracture sets with the wells GPK2, GPK3 and GPK4. Four sets of 2000 discs are randomly generated in a parallelepiped volume of 15 km³ (dimension: E-W = 2 km ; N-S: 3 km; vertical: 2.5 km – equal to the volume taken into account in the numerical model, Gentier *et al.*, 2011). The direction and the dip of all discs of a given set are the mean values of those determined for each set of fractures.

Several fracture radii have been tested, from infinite to 50 m, so that a volumetric density is estimated as a function of fracture lengths. The number of discs of each set that intersect each well (GPK2, GPK3 and GPK4) between -3500 m NGF and its bottom is then counted. The previous procedure is repeated for six times to obtain a sequence of random draws. The proportion of intersections corresponds to the probability of intersection. The probability in a scenario of infinite discs is given Table 2. As a result, it appears that the probability of intersection of the wells with a fracture set lies within a large interval values. For example, as illustrated Figure 3, for a fracture of the F3 set, the probability of intersection is very low with GPK2 (3%) and significantly higher with GPK3 and GPK4 (respectively 22% and 37%). Globally, the GPK2 trajectory is mainly favorable to intersect the fracture sets NNW-SSE striking W dipping (F2) and NW-SE striking (F4); the probability of intersection with a fracture set with direction N-S striking E dipping (F1) and NE-SW striking (F3) is around 8% and 3%, respectively. The GPK3 trajectory is favorable to intersect with an equal probability the fracture sets N-S to NNW-SSE striking (F1 and F2) and NE-SW striking (F3); NW-SE striking (F4) is a little bit less favorably oriented. The GPK4 trajectory is favorable to intersect with an equal probability the fracture sets

with directions N-S to NE-SW striking (F1 and F3); it is less favorable to intersect fractures with directions NW-SE to NNW-SSE striking W dipping (F4 and F2).

Note that the wells trajectories are not rectilinear. The probability of intersection varies then with depth generating high concentration of fractures in limited depth intervals associated with well orientation.

The density d of fractures in the studied volume V is then estimated from the probability p of intersection of each set of discs with the trajectory of each well and the number n of observed

Table 2. Probability of intersection of sets of discs with the wells.

Probab. [%] of intersection	of	fracture sets with strike :			
	With	N 0° (~F1)	N 160° (~F2)	N 40° (~F3)	N 130° (~F4)
GPK2	8 +/-1	33 +/-2	3 +/-1	20 +/-2	
GPK3	24 +/-2	24 +/-2	22 +/-3	16 +/-1	
GPK4	31 +/-2	23 +/-2	37 +/-2	10 +/-1	

fractures in GPK3 and GPK4 (no observation is available for GPK2): $d = \frac{n}{V}$.

These density/radius couples offer an infinity of solutions that allow the reproduction of the linear density observed along the wells. The Soultz-sous-Forêts granitic basement has undergone

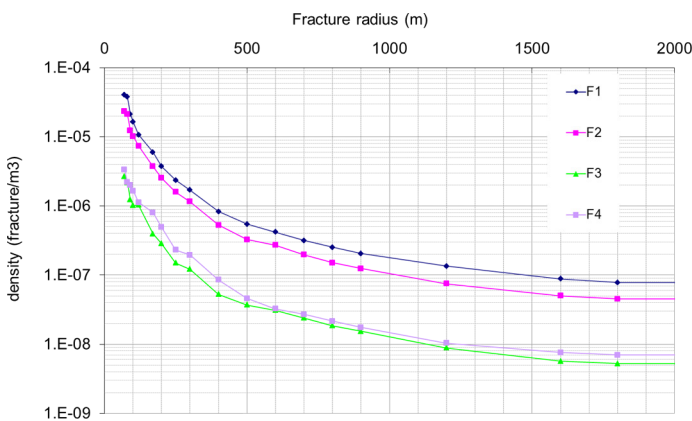


Figure 7. Densities for each fracture set.

many tectonic deformations; it thus can be considered as a completely blocky rock mass. In such a rock mass, all fractures are terminated at other fractures and higher the fracture density is, lesser the fracture size is. In the case of Soultz-sous-Forêts basement, the assumption of highly “split” fracture network can thus be made. The fractures radii are thus probably relatively small, from decametric to hectometer scale.

The presented density is a first estimation that is adjusted with hydraulic arguments based on the modeling of the Soultz-sous-Forêts EGS hydraulic behavior; this work is detailed in the companion paper referred as Gentier *et al.* (2011).

Conclusion

The construction of a 3D fracture network is performed from the available data on the site resulting from the observations done in boreholes (1D data). About 6000 fractures have been

identified, located and measured by borehole imagery techniques (strike and dip measured on a few squared centimeters section of the fracture intercepted by the well bore). These data cannot be directly used to estimate the efficient hydraulic network because of several biases: uncertainties and unknowns due to wells trajectories, detection method and to the fact that the efficient hydraulic fracture network is a subset of the fracture network. Some biases can be corrected by statistical and probabilistic methods as the orientation sampling bias due to linear sampling using the Terzaghi’s correction factor. But we show that this method is limited when the fracture is nearly parallel to the well axis. To avoid the linked uncertainties, the Fisher distribution method has been used to highlight four main fracture sets, and a fifth uniform fracture set has been defined. The fractures with low probability of intersection are thus taken into account, which is in some respects geologically consistent. The five fracture sets can be related to one or multiple tectonic events.

The 3D fracture network is characterized by fracture shape, length and density. We first make the assumption of circular shaped fractures. A spatial homogeneous distribution of fractures is considered. Couples density/length are then defined from 1D observed density and probability of intersection estimation. The fracture length cannot be limited by direct observations, but as the granite of Soultz-sous-Forêts has been deformed by numerous tectonic phases, we can make the assumption that the fracture network is highly split and that fracture length is around hectometer scale.

Some parameters as number, orientation characteristics and density/length couples of fracture set that are needed to construct the efficient hydraulic fracture network are thus estimated with statistical computation and geological constraints. But important uncertainties still remain. The most important question deals with the proportion of detected fracture that are permeable.

This 3D fracture network will be used to model the Soultz-sous-Forêts EGS reservoir hydraulic behavior, using Discrete Fracture Network (DFN) approach.

Acknowledgements

This work was supported by the EGS Pilot Plant project within the sixth framework program of the European Community and by Ademe (French Environment and Energy Management Agency). The authors would like to thank the staff of the EEIG Heat-Mining for their assistance and the persons in charge of the UBI data treatment at BRGM, in particular Chrystel Dezayes.

References

- Bergerat, F., 1985, “Déformations cassantes et champs de contraintes tertiaires dans la plateforme européenne”, Ph.D. thesis, Université Pierre & Marie Curie, Paris VI.
- Billiaux D., 1990, “Hydrogéologie des milieux fracturés : géométrie connectivité, et comportement hydraulique”, Documents du BRGM n°186, 220 p.
- Dezayes C., B. Valley, E. Maqua, G. Syren, A. Genter, 2005a, “Natural fracture system of the Soultz granite based on UBI data in the GPK3 and GPK4 wells”, EHDRA scientific meeting, March 05, 11 p.
- Dezayes .C., A. Genter , GR. Hooijkaas, 2005b, “Deep-Seated Geology and Fracture System of the EGS Soultz Reservoir (France) based on Recent 5km Depth Boreholes”, Proceedings World Geothermal Congress 2005, Antalya, Turkey, 24-29 April 2005, 6p.

- Edel J. B., K. Schulmann, and Y. Rotstein, 2006, "The Variscan tectonic inheritance of the Upper Rhine Graben: evidence of reactivations in the Lias, Late Eocene-Oligocene up to the recent", *International Journal of Earth Sciences*, p.305-325
- Fisher, R. A., 1953, "Dispersion on a sphere" *Proc. Roy. Soc. London, Ser. A*, v.217, p. 295-305
- Genter A., C. Castaing, C. Dezayes, H. Tenzer, H. Traineau and T. Villemin, 1997, "Comparative analysis of direct (core) and indirect (borehole imaging tools) collection of fracture data in the Hot Dry Rock reservoir (France)", *J. Geoph. Res.*, v.102, B7, p.15419-15431.
- Gentier S., E. Lamontagne, C. Archambault, J. Riss, 1997, "Anisotropy of flow in a fracture undergoing shear and its relationship to the direction of shearing and injection pressure", *Int. J. Rock Mech. & Min. Sci.* 34:3-4, paper No. 094., 12p.
- Gentier S., X. Rachez, M. Peter-Borie and A. Blaisonneau, 2011, "Transport and flow modelling of the deep geothermal exchanger between wells at Soultz-sous-Forêts (France)", *Proceedings of Geothermal Resources Council 2011, San Diego*, 12p.
- Hurtig, E., V. Cermak, R. Haenel and V. Zui, 1992, "Geothermal atlas of Europe." *Hermann Haak Verlagsgesellschaft mbH, Germany*.
- Priest, S.D., 1993, "Discontinuity Analysis for Rock Engineering". Chapman and Hall, London, p71-93.
- Schumacher ME., 2002, "Upper Rhine Graben: role of pre-existing structures during rift evolution" *Tectonics*, v. 21(1).
- Terzaghi, R. D., 1965, "Sources of errors in joint surveys", *Geotechnique*, v.15, p.287- 304.
- Villemin, T., 1986, "Tectonique en extension, fracturation et subsidence : Le Fossé Rhénan et le bassin de Sarre-Nahe.", *Ph.D. thesis, Paris VI*, 270 pp.
- Valley, B. C., 2007, "The relation between natural fracturing and stress heterogeneities in deep-seated crystalline rocks at Soultz-sous-Forêts (France)." *EHT PhD thesis*, 260 pp.
- Yow, J.L., 1987, "Blind zones in the acquisition of discontinuity orientation data". *International Journal of Rock Mechanics and Mining Sciences and Geomechanics Abstracts. Technical Note. v.24: 5, p.317-318.*
- Ziegler, P.A., 1990, "Geological Atlas of Western and Central Europe", *Shell Int. Pet. Maatschappij, Geol. Soc. Publ. House, Bath, UK*, 239 pp.

